Photochromic Behavior and Diastereomeric Isomerism in [(η^6-spirobenzopyran)RuCp*]PF_6

Akihiro Moriuchi, Kazunori Uchida, Akiko Inagaki, and Munetaka Akita*

Chemical Resources Laboratory, Tokyo Institute of Technology, R1-27, 4259 Nagatsuta, Midori-ku, Yokohama 226-8503, Japan

Received August 4, 2005

Complexation of photochromic spirobenzopyran **1** (SP-X) with the labile cationic ruthenium complex [Cp*Ru(NCMe)$_3$]PF_6 (**2**) furnishes two isomers of the η^6-arene adducts, [Cp*Ru(η^6-SP-X)]PF_6 (**3** and **4**), i.e., one of the two diastereomeric adducts of the indoline part in the closed form of **1** (**3**) and the adduct of the dihydrobenzopyran part in the open *trans*-merocyanine form of **1** (**4**). UV irradiation of the pale yellow adduct **3** does not cause an apparent color change, but ^{1}H NMR monitoring reveals formation of the diastereomer **3′** with the inverted configuration of the chiral spiro carbon atom, which gradually reverts to **3** when left at ambient temperature in the dark over the course of a few days. The two diastereomers **3/3′** are interconverted with each other through the open, merocyanine form **III**, which should result from photochemical C−O bond heterolysis of **3/3′**. In the case of the SP-H complex **3b**, photochromic behavior (**3b** ↔ **III′b** (trans isomer of **IIIb**)) is noted but the amount of the colored species **III′b** formed is limited. On the other hand, irradiation of the deep red isomer **4** with visible light brings about trans to cis isomerization of the olefinic part to result in complete conversion to an equilibrated mixture of the two diastereomeric closed species **5** and **5′**, which are interconverted with each other at ambient temperature via the transient cis-open intermediate **II**. UV irradiation of the equilibrated mixture **5/5′** reverses the ring-opening process to give a photoequilibrated mixture containing **4** in addition to **5/5′**. Thus, **3** and **4** undergo interconversion of the diastereomers via photochemical C−O bond heterolysis and photochromic behavior is noted for **4**.

Introduction

Much attention has been focused on photochromic compounds, because various physicochemical properties of them, in particular, color, can be switched by the action of electromagnetic radiation and/or heat.[1] Combination with other chemical auxiliaries is expected to lead to a new phase of the chemistry, and various attempts have been made to add some more sophisticated functions.

Spirobenzopyran (SP; **1**) is one of the most extensively studied photochromic compounds (Scheme 1).[1] UV irradiation of **1** causes C−O bond heterolysis of the central spiro carbon atom moiety to convert the tetrahedral sp^3-hybridized spiro carbon atom into the planar sp^2-hybridized carbon atom, through which the separated aromatic systems (A and B rings) are conjugated with each other to exhibit absorptions in the visible region (**1′**; merocyanine form). (For simplicity's sake, the aromatic rings of the indoline and benzopyran moieties in **1** are denoted as A and B rings, respectively.) The reverse ring-closing process is promoted by irradiation of visible light or heat. While complexation of the highly functionalized SP-X molecules with metal species should be a promising method for the introduction of a new function,[2,3] few studies on combination with an organometallic system have been carried out and, in particular, little is known about the behavior of η^6-coordinated spirobenzopyran complexes.[3] Herein we wish to report formation of cationic (η^6-spirobenzopyran)RuCp* complexes[4] and their photochromic behavior and stereochemical isomerism.

(1) Bamfield, P. *Chromic Phenomena, Technological Applications of Color Chemistry*; Royal Society of Chemistry: Cambridge, U.K., 2001. Dürr, H.; Bouas-Laurent, H. *Photochromism: Molecules and Systems*; Elsevier: Amsterdam, 2003. The special thematic issue of *Chem. Rev.* for "Photochromism: Memories and Switches−Introduction": *Chem. Rev.* **2000**, *100*, 1683−1890.

(2) Photochemical properties of spirobenzopyrans with a chelating moiety (e.g. a crown ether tether) have been studied to a considerable extent: Atabekyan, L. S.; Chibisov, A. K. *J. Photochem.* **1986**, *34*, 323. Kimura, K.; Yamashita, T.; Yokoyama, M. *J. Chem. Soc., Perkin Trans. 2* **1992**, 613. Atabekyan, L.; Chibisov, A. *Mol. Cryst. Liq. Cryst. Sci. Technol., Sect. A: Mol. Cryst. Liq. Cryst.* **1994**, *246*, 263. Atabekyan, L. S.; Lilikin, A. I.; Zakharova, G. V.; Chibisov, A. K. *High Energy Chem.* **1996**, *30*, 409. Kimura, K.; Teranishi, T.; Yokoyama, M. *Supramol. Chem.* **1996**, *7*, 11. Filley, J.; Ibrahim, M. A.; Nimlos, M. R.; Watt, A. S.; Blake, D. M. *J. Photochem. Photobiol., A: Chem.* **1998**, *117*, 193. Gorner, H.; Chibisov, A. K. *J. Chem. Soc., Faraday Trans.* **1998**, *94*, 2557. Collins, G. E.; Choi, L.-S.; Ewing, K. J.; Michelet, V.; Bowen, C. M.; Winkler, J. D. *Chem. Commun.* **1999**, 321. Kimura, K.; Sakamoto, H.; Kado, S.; Arakawa, R.; Yokoyama, M. *Analyst* **2000**, *125*, 1091. Nakamura, M.; Fujioka, T.; Sakamoto, H.; Kimura, K. *New J. Chem.* **2002**, *26*, 554. Bulanov, A. O.; Luk'yanov, B. S.; Kogan, V. A.; Stankevich, N. V.; Lukov, V. V. *Russ. J. Coord. Chem.* **2002**, *28*, 46. Querol, M.; Bozic, B.; Salluce, N.; Belser, P. *Polyhedron* **2003**, *22*, 655. Liu, S. *Mol. Cryst. Liq. Cryst.* **2004**, *419*, 97. Kimura, K.; Sakamoto, H.; Uda, Ryoko M. *Macromolecules* **2004**, *37*, 1871.

(3) To our knowledge, (η^6-SP)Cr(CO)$_3$ is the only previously reported example of a η^6-SP-X complex. Formation of the A ring adducts, their photochromism (half-life of the colored species ≤10 min), and diastereoisomerism including exclusive formation of one of the two diastereomers upon UV irradiation were reported: Miyashita, A.; Iwamoto, A.; Kuwayama, T.; Shitara, H.; Aoki, Y.; Hirano, M.; Nohira, H. *Chem. Lett.* **1997**, 965.

10.1021/om0506771 CCC: $30.25
Publication on Web 11/08/2005

Scheme 1

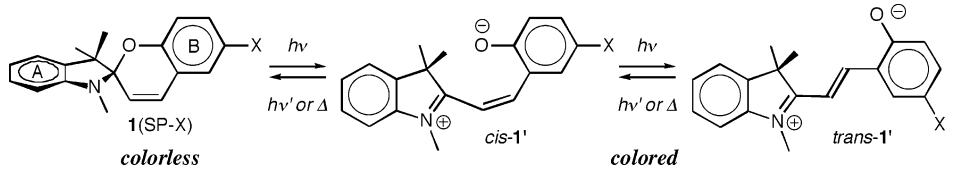

Scheme 2

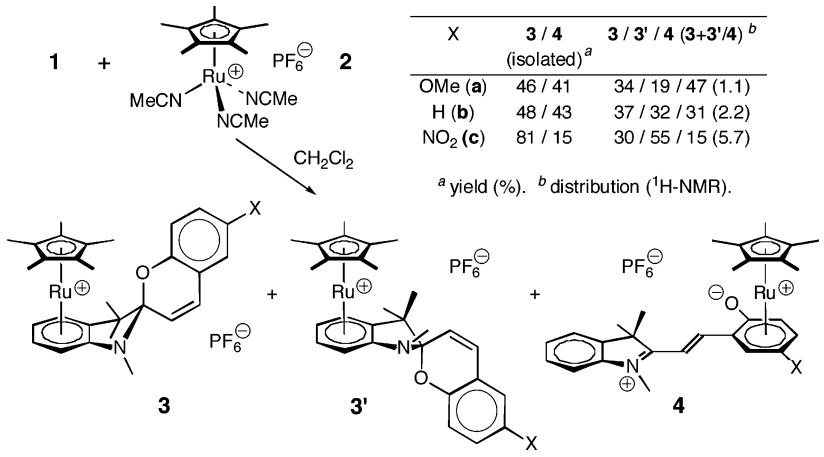

X	3 / 4 (isolated)[a]	3 / 3′ / 4 (3+3′/4)[b]
OMe (**a**)	46 / 41	34 / 19 / 47 (1.1)
H (**b**)	48 / 43	37 / 32 / 31 (2.2)
NO_2 (**c**)	81 / 15	30 / 55 / 15 (5.7)

[a] yield (%). [b] distribution (^{1}H-NMR).

Results and Discussion

Preparation and Characterization of Cationic Spirobenzopyran−RuCp* Adducts. (i) Preparation. Treatment of spirobenzopyrans (**1**; SP-X) with the labile cationic ruthenium species $[Cp^*Ru(NCMe)_3]PF_6$ (**2**)[4h] in CH_2Cl_2 afforded a mixture of two isomeric adducts, $[Cp^*Ru(\eta^6\text{-SP-X})]PF_6$ (**3**, pale yellow; **4**, deep red), which were separated by column chromatography (Scheme 2).[5] While formation of **3′** (a diastereomer of **3**) was detected by ^{1}H NMR analysis of reaction mixtures, **3′** was converted to **3** during chromatographic separation and, therefore, **3′** could not be isolated from the reaction mixtures. (**3′** could be obtained by UV irradiation of **3** as described below.) It was noted that, as X becomes more electron withdrawing, the **3/4** ratio increases (**a**, 1.1; **b**, 2.2; **c**, 5.7).

(ii) Spectroscopic Characterization. Many isomeric structures are possible for the η^6 adducts. As for the closed species (adducts of **1**), the two aromatic rings A and B in **1** are susceptible to η^6 coordination and, furthermore, the chiral spiro carbon atom makes the two adducts resulting from coordination of the two faces of the aromatic ring diastereomeric, leading to four isomers. As for the open species (adducts of **1′**), addition to the two aromatic rings (A and B) in the cis and trans isomers can form four isomers. Of the eight candidates, three (**3**, **3′** and **4**) are formed from **1** and **2**, and another isomer **5** is derived from **4**, as described below.

The adduct formation is readily confirmed by ESI-MS and ^{1}H NMR spectra, and the site of the coordination can be determined on the basis of the signals, which are shifted to higher field upon complexation. The upfield shift is regarded as being diagnostic of η^6 coordination of an arene molecule.[4b−h] As typical examples, ^{1}H NMR spectra (aromatic region) of the SP-NO_2 derivatives **1c**, **3c**, and **4c** are compared as shown in Figure 1. The ^{1}H NMR signals at lower field can be assigned to the A and B rings and the olefinic part on the basis of decoupling and 2D experiments and the coupling patterns (1,2-disubstitution (A ring) vs 1,2,4-trisubstitution (B ring)). For **3c**, complexation causes

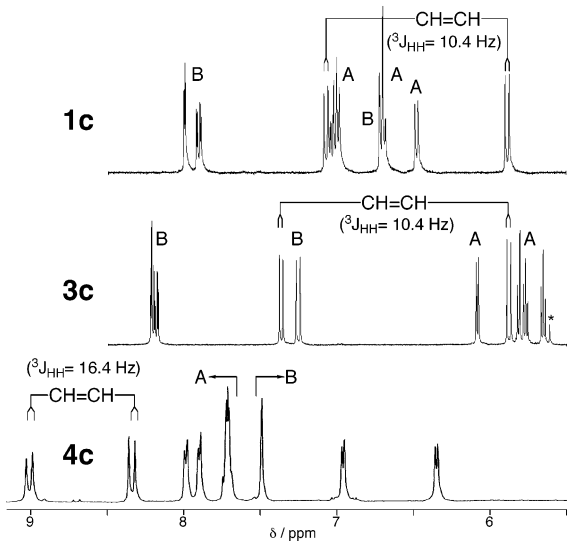

Figure 1. Comparison of ^{1}H NMR spectra for **1c**, **3c**, and **4c** observed at 400 MHz in acetone-d_6. The asterisk denotes residual CH_2Cl_2.

(4) (a) Kündig, E. P. *Transition Metal Arene π-Complexes in Organic Synthesis and Catalysis*; Springer: Berlin, 2004. For $[Cp^*Ru(\eta^6\text{-arene})]^+$ complexes, see, for example: (b) Fagan, P. J.; Ward, M. D.; Calabrese, J. C. *J. Am. Chem. Soc.* **1989**, *111*, 1698. (c) Schrenk, J. L.; McNair, A. M.; McCormick, F. B.; Mann, K. R. *Inorg. Chem.* **1986**, *25*, 3501. (d) He, X. D.; Chaudret, B.; Dahan, F.; Huang, Y.-S. *Organometallics* **1991**, *10*, 970. (e) Vichard, D.; Gruselle, M.; Amouri, H. E.; Jaouen, G.; Vaissermann, J. *Organometallics* **1992**, *11*, 976. (f) Seiders, T. J.; Baldridge, K. K.; O'Connor, J. M.; Siegel, J. S. *J. Am. Chem. Soc.* **1997**, *119*, 4781. (g) Pasch, R.; Koelle, U.; Ganter, B.; Englert, U. *Organometallics* **1997**, *16*, 3950. (h) Steinmetz, B.; Schenk, W. A. *Organometallics* **1999**, *18*, 943.

(5) Treatment of **1b** with an excess amount of **2** (>2 equiv) furnished a 1/2 adduct, as characterized by ESI-MS and ^{1}H NMR spectra. The ^{1}H NMR suggested formation of a mixture of isomers, which could not be separated.

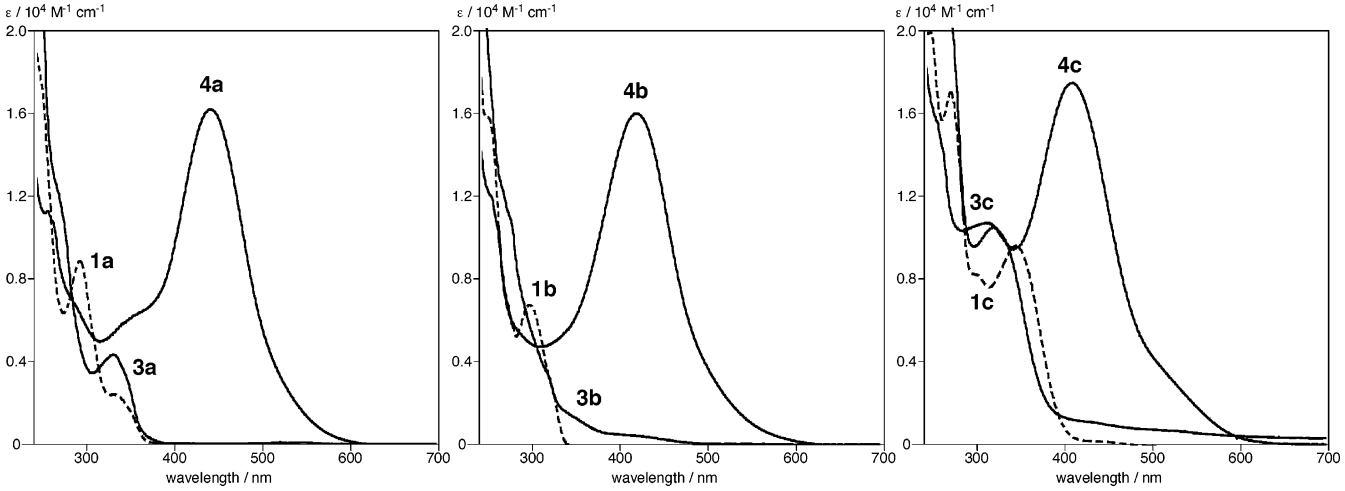

Figure 2. UV−visible spectra for **1**, **3**, and **4** (in CH_2Cl_2). Concentrations: [**1a**] = 3.10×10^{-5} M, [**3a**] = 2.49×10^{-5} M, [**4a**] = 2.49×10^{-5} M, [**1b**] = 2.49×10^{-5} M, [**3b**] = 2.50×10^{-5} M, [**4b**] = 2.72×10^{-5} M, [**1c**] = 2.50×10^{-5} M, [**3c**] = 2.50×10^{-5} M, [**4c**] = 2.50×10^{-5} M,

Chart 1

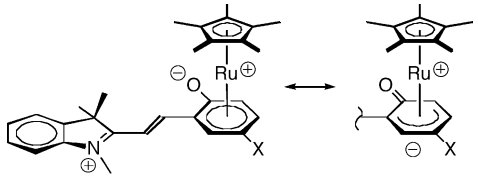

upfield shifts of the signals attributed to the A ring, while a significant shift is not noted for the remaining signals attributed to the B ring and the CH=CH moiety. In combination with (i) the similar coupling constants ($^3J_{HH}$) observed for the CH=CH linkage for **1c** and **3c** (10.4 Hz) indicative of a cis arrangement[6] and (ii) upfield shifts of the ^{13}C NMR signals of the coordinated A ring, it is concluded that complex **3c** results from addition to the A ring in the closed form of **1c**. Although the orientation of the SP-NO_2 ligand (stereochemistry of the spiro carbon atom) cannot be determined by the spectroscopic data alone, X-ray crystallography (see below) reveals the orientation of the pyran oxygen atom being directed to the Ru side.

On the other hand, the upfield-shifted ^1H (Figure 1) and ^{13}C NMR signals for **4c** are assigned to the B ring, indicating coordination of the B ring. The red color suggests formation of a merocyanine structure (**1′** type; Scheme 1), which is supported by the configuration of the olefinic part, determined to be trans on the basis of the $^3J_{HH}$ coupling constant for the CH=CH part. The value (16.4 Hz)[6] is substantially larger than those of the closed forms **1c** and **3c** (see above). The zwitterionic merocyanine form is also consistent with the rather intense IR absorption at 1607 cm^{-1}, attributable to a C−O vibration. The double-bond character of the C−O part should result from contribution of a η^5-cyclohexadienonyl coordination of the phenoxy group (**4′**; Chart 1), as indicated by the crystallographic structure determination (see below).

Similar spectroscopic features observed for the compounds of the **a** and **b** series are also consistent with the formulation shown in Scheme 2.

(6) Pretsch, P. D.; Seible, J.; Simon, W.; Clerc, T. *Strukturaufklälung organischer Verbindungen,* 2nd ed.; Springer: Berlin, 1981.

Ring opening−closing (**3** vs **4**) is also evident from UV−vis spectra (Figure 2). As can be seen from the spectra, the closed species **3** (λ_{max}/nm (ϵ/M^{-1} cm^{-1}): 328 (4.3×10^3) (**3a**); featureless (**3b**); 264 (2.22×10^4), 318 (1.05×10^4) (**3c**)) do not show any characteristic absorption in the visible region in a manner similar to that for SP-X **1** (λ_{max}/nm: 322 (**1a**); 322 (**1b**); 326 (**1c**)),[14] while the open species **4** show intense absorptions around 400 nm (λ_{max}/nm (ϵ/M^{-1} cm^{-1}): 441 (1.62×10^4) (**4a**); 420 (1.59×10^4) (**4b**); 312 (1.07×10^4), 406 (1.73×10^4) (**4c**)), which are comparable to those for the merocyanine forms **1′** (λ_{max}/nm: 406 (**1′a**); 394 (**1′b**); 580 (**1′c**))[14] and the O-protonated merocyanine (cf. the N−CH_2CH_2OH derivative of **1′b**: λ_{max} 563 nm).[7a] As the substituent (X) on SP-X becomes electron withdrawing, the absorption maximum is shifted to higher energies, while the absorption coefficients are comparable. The hypsochromic shift suggests that the absorptions are due to LMCT.

(iii) Crystallographic Characterization. The molecular structures of **3a**,**c** and **4c** have been determined by X-ray crystallography (Figure 3), and for comparison, the diastereomeric species **3′b** (see below) is discussed in this section as well. The low quality of the crystals of **4c**[8] and the disorder noted for the five-membered

(7) (a) Godsi, O.; Peskin, U.; Kapon, M.; Natan, E.; Eichen, Y. *Chem. Commun.* **2001**, 2132. (b) Raymo, F. M.; Giordani, S.; White, A. J. P.; Williams, D. J. *J. Org. Chem.* **2003**, *68*, 4158.

(8) Because the quality of the single crystals of **4c** was poor, only the preliminary result is shown here. Crystallographic data for **4c**: $C_{29}H_{33}N_2O_3F_6PRu$, formula weight 703.63, monoclinic crystal system, space group *C*2/*c*, a = 26.33(9) Å, b = 11.29(4) Å, c = 26.39(10) Å, β = 122.3(2)°, V = 6638(42) Å^3, Z = 8, T = −60 °C, d_{calcd} = 1.408, μ = 0.584 mm^{-1}, current R1 = 0.1160 for 1016 reflections with $I > 2\sigma(I)$, wR2 = 0.3008 for all observed 2887 reflections with 174 parameters (isotropic refinements for all non-hydrogen atoms; H atoms not included in the refinement).

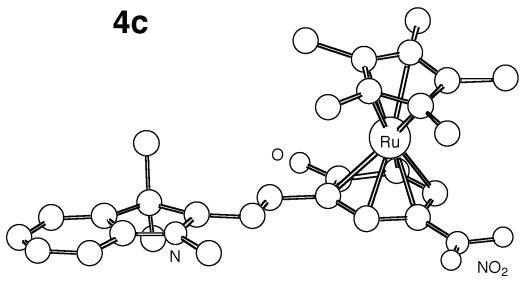

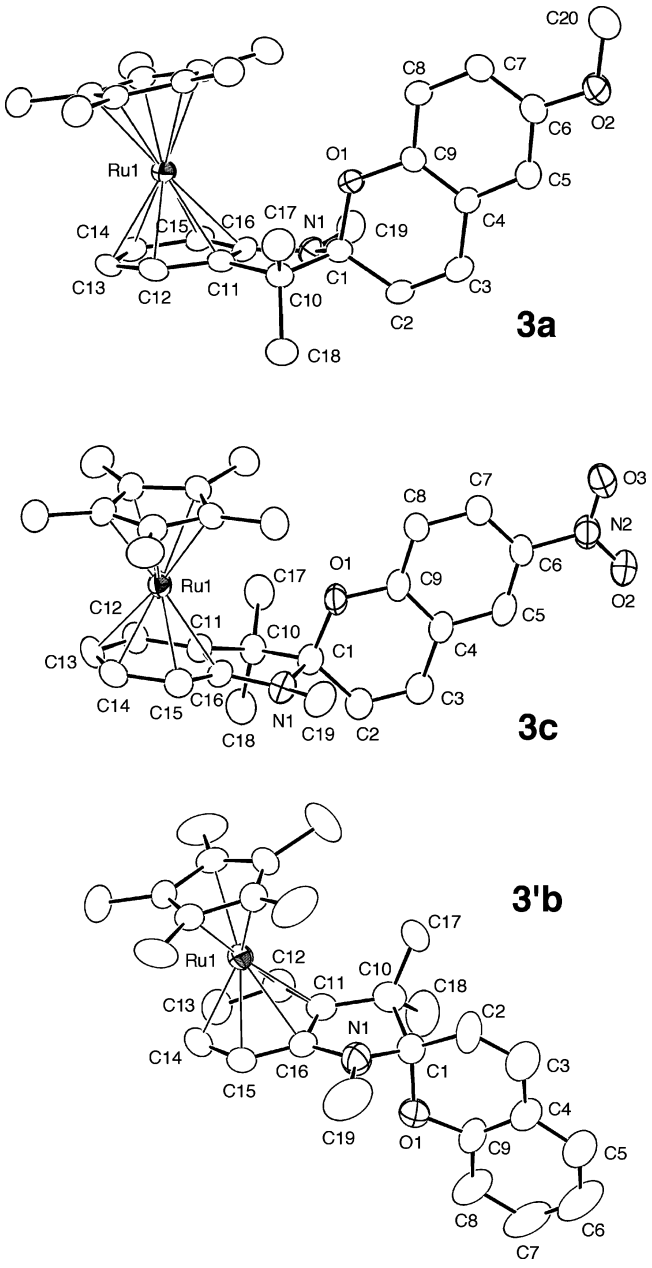

Figure 3. Molecular structures of **3a**,**c** and **3′b** drawn with thermal ellipsoids at the 30% probability level.

dihydropyrrole ring (NMe ↔ CMe_2) in **3′b**[9] hamper a detailed discussion of them.

Typical η^6-arene coordination of the A ring is evident for **3a,c** and **3′b**. Because, however, the C16 atoms are always located farthest from the ruthenium atom (**3a**, Ru1−C14 = 2.190(5) Å, Ru1−C16 = 2.339(4) Å; **3c**, Ru1−C14 = 2.189(6) Å, Ru1−C16 = 2.334(5) Å; **3′b**, Ru1−C14 = 2.18(1) Å, Ru1−C16 = 2.296(9) Å), π-donation from the N1 atom should distort those parts toward η^5-cyclohexadienyl structures. No significant substituent

Chart 2

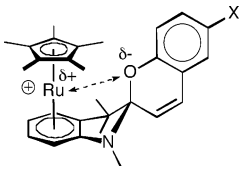

effect of R (**3a** vs **3c**) is noted. On the other hand, the Ru···C(=O) separation (2.47(3) Å) for **4c** exceeding the distance for a Ru−C bonding interaction (the other Ru−C distances are 2.11−2.23 Å) indicates significant contribution of a η^5-cyclohexadienonyl structure, which is consistent with the appearance of the $\nu_{C=O}$ vibration discussed above (Chart 1). Such a distortion should result from the push−pull effects of the negative charge on the phenolate oxygen atom and the electron-withdrawing NO_2 and RuCp* groups.

Stereochemistry of the chiral spiro carbon atoms (C1) in **3a**,**c** and **3′b** and the olefinic moiety in **4c** is verified by X-ray crystallography. In **3a**,**c** the O1 atoms are directed to the Ru side, whereas the inverted configuration is observed for **3′b**. The trans configuration of the olefinic part in **4c** is consistent with the large $^3J_{HH}$ coupling constants (see above).[10]

When the structures of **3a**,**c** and **3′b** are inspected in detail, a difference is noted for the conformation of the indoline moiety. The puckering of the N-containing five-membered ring is opposite for **3** and **3′**, as is evident from the dihedral angle made by the N1−C16−C11−C10 and N1−C1−C10 planes (θ_1 = 21.8° (**3a**), 22.4° (**3c**), −28.4° (**3′b**)). In the CSD database 16 spirobenzopyrans, including **1a**,**c**, are listed, and all of them adopt conformations similar to that of **3** (e.g. **1a**: 35.1°).[11] The oxygen atom in the benzopyran ring occupies the axial position of the puckered N-containing five-membered ring ($\mathbf{1_{ax}}$), presumably due to the repulsion between the olefinic hydrogen atom on C2 and the methyl group of the CMe_2 moiety. The θ_1 values for **3** being smaller than that of **1** are indicative of some steric repulsion between the RuCp* moiety and the lone pair of electrons on O1. Despite such an apparent repulsive interaction in **3**, the O1 atom is still directed to the Ru atom ($\theta_1 > 0$; Ru1···O1 separations 3.907(3) Å (**3a**) and 4.003(4) Å (**3c**)), indicating some electrostatic attractive interaction between them (Chart 2). However, no coordinating interaction is feasible because of the coordinatively saturated electronic configuration at the Ru atom.

(iv) Selectivity on Formation of the Adducts 3/3′/4. The dependence of the **3/4** ratio (isolated samples) is noted as described above (Scheme 2). Because, however, **3′** is isomerized to **3** during the separation process, the product distribution has been determined by ^{1}H NMR analysis of the reaction mixture and the results are also shown in Scheme 2. It is revealed that, as X becomes more electron donating, (i) the (**3** + **3′**)/**4** ratio decreases and (ii) the **3**/**3′** ratio increases.

(9) Complex **3b** was also characterized by X-ray crystallography, but the molecule sitting on a crystallographic symmetrical site is completely disordered with respect to the mirror plane bisecting the coordinated arene ring. Although a molecular structure similar to that of **3a**,**c** can be confirmed, the result is not included. Crystallographic data for **3b**: $C_{29}H_{34}NOF_6PRu$, formula weight 658.63, monoclinic crystal system, space group $P2_1/m$, a = 10.2078(6) Å, b = 11.477(1) Å, c = 13.561(1) Å, β = 91.456(5)°, V = 1588.3(2) Å^3, Z = 2, T = −60 °C, d_{calcd} = 1.377, μ = 0.600 mm^{-1}, current R1 = 0.104 for 3213 reflections with $I > 2\sigma(I)$, wR2 = 0.303 for all observed 3620 reflections with 240 parameters.

(10) The open forms of free SP-X molecules were also characterized by X-ray crystallography.[7]

(11) **1a**: Raic-Malic, S.; Tomaskovic, L.; Mrvos-Sermek, D.; Prugovecki, B.; Cetina, M.; Grdisa, M.; Pavelic, K.; Mannschreck, A.; Balzarini, J.; De Clercq, E.; Mintas, M. *Bioorg. Med. Chem.* **2004**, *12*, 1037. **1c**: Karaev, K. Sh.; Furmanova, N. G.; Belov, N. V. *Proc. Natl. Acad. Sci. USSR* **1982**, *262*, 877. Clegg, W.; Norman, N. C.; Flood, T.; Sallans, L.; Kwak, W. S.; Kwiatkowski, P. L.; Lasch, J. G. *Acta Crystallogr., Sect. C: Cryst. Struct. Commun.* **1991**, *47*, 817.

Scheme 3

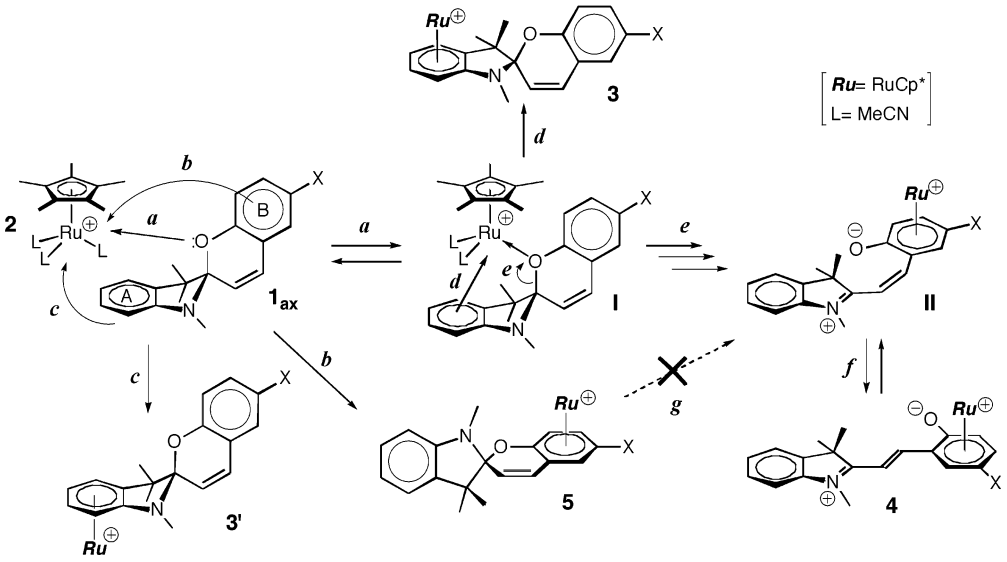

These two trends can be interpreted in terms of a combination of electronic and steric considerations (Scheme 3). Three pathways are feasible for the initial interaction between **1** and **2**: i.e., interaction with the lone pair of electrons on O (path *a*) and with the aromatic rings (paths *b* and *c*) leading to **I**, **5**, and **3′**, respectively.

In the case of **1a**, the electron-donating OMe group on the B ring enhances the electron density at the O atom of the dihydrobenzopyran ring through π-donation so as to promote coordination of the O atom to the Cp*Ru center (path *a*). Subsequent coordination of the A ring in **I** gives **3** (path *d*), while heterolytic C−O bond cleavage followed by coordination of the B ring results in the zwitterionic intermediate **II** (path *e*), where olefin isomerization finally leads to **4** (path *f*). On the other hand, direct interaction with the B ring is also feasible (path *b*), because the electron density of the B ring is also enhanced by the OMe group. This route, however, can be ruled out, because the resultant species **5** (formed via irradiation of **4** with visible light; see below) does not undergo isomerization to **4** (path *g*) under thermal reaction conditions.[12] In path *c*, taking into account the stable conformer of **1** (**1_{ax}**; see above), the Ru fragment should approach from the bottom side so as to avoid steric interaction with the dihydrobenzopyran ring; as a result, **3′** should be formed. Judging from the observed product distribution (**3a** + **3′a** > **4a**; **3a** > **3′a**), the dominant formation route of the SP-OMe complexes involves O coordination (path *a* leading to **I**) rather than direct coordination (path *c* leading to **3′c**) and, from **I**, the κ^1-to-η^6 slippage on the B ring (path *e* leading to **4**) associated with C−O bond heterolysis is slightly preferable to the O(κ^1) to A ring (η^6) shift (path *d* leading to **3**).

On the other hand, in the case of **1c**, the electron-withdrawing NO_2 group should lower the electron density at the O atom and, therefore, the direct interaction (path *c*) should be the dominant reaction pathway to afford **3′** as the major product.

(12) The open form **5** was not converted to the closed form **4** under thermal reaction conditions but upon UV irradiation (see below).

Photochemical Behavior of the Cp*Ru(η^6-SP-X) Cations. The synthetic study of the adducts **3** and **4** was followed by a study of their photochemical properties.

(i) Photochemical Behavior of 3. UV irradiation of **3** caused no significant color change, but ^{1}H NMR analysis revealed the occurrence of conversion to the new species **3′** (Scheme 4). The ratios of the species present in the equilibrated mixtures (**3**/(**3** + **3′**)) are also summarized in Scheme 4. Photostationary equilibrated states were attained after irradiation for 2−3 h, and a solvent effect was noted. No deterioration was observed for the SP-H (**3b**) and -OMe complexes (**3a**), while the SP-NO_2 complex **3c** decomposed upon prolonged UV irradiation.

As a typical example, ^{1}H NMR and UV−vis spectral changes of the SP-H complex **3b** are shown in Figures 4 and 5, respectively. After 40 min of irradiation, a set of new ^{1}H NMR signals appeared and, after 2 h of irradiation, the signals for **3b** were almost completely replaced by those of **3′b** (Figure 4). When the equilibrated samples of **3/3′b** were left at ambient temperature, the mixture slowly reverted to **3b** over the course of 3−4 days. On the other hand, UV−vis monitoring revealed formation of a minor colored species, which could not be detected by ^{1}H NMR (Figure 5). Irradiation for 30 min caused appearance of weak bands at 433 and 550 nm. Upon further irradiation the transient weak absorptions disappeared and, after 2−3 h, a UV−vis spectrum similar to that of **3b** was obtained (Figure 5a). It should be noted, however, when the irradiation was switched off after appearance of the weak bands, they were retained and the half-life of the intermediate was longer than 2 days (Figure 5b). The colored species was detected only for **3b**, and no colored species could be detected for **3/3′a**,**c**.

These spectral changes reveal that (1) the new species **3′** formed by UV irradiation of **3** is an isomer of **3** with a closed structure and (2) **3′** reverts to **3** under thermal reaction conditions. Furthermore, in the case of **3b**, (3) a colored species is detected by UV−vis spectroscopy and (4) not only the coloration but also the decoloration is promoted by UV irradiation.

Scheme 4

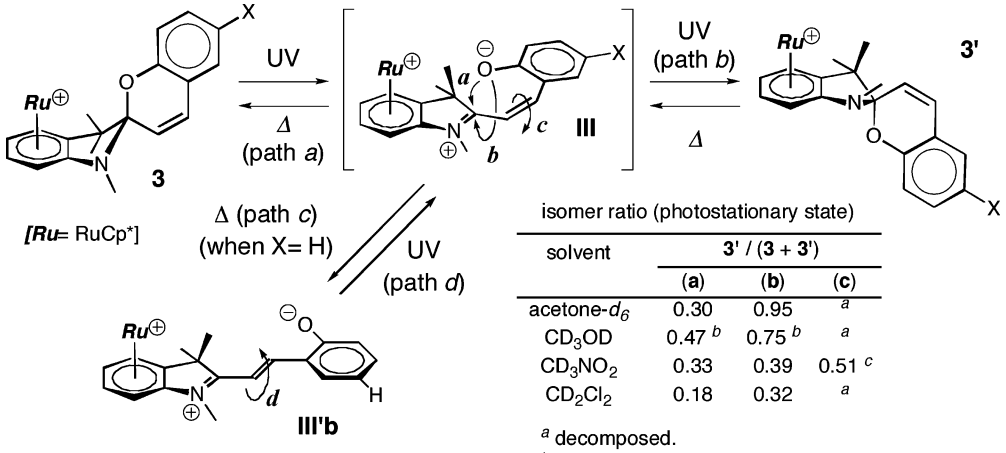

isomer ratio (photostationary state)

solvent	3' / (3 + 3')		
	(a)	(b)	(c)
acetone-d_6	0.30	0.95	[a]
CD_3OD	0.47 [b]	0.75 [b]	[a]
CD_3NO_2	0.33	0.39	0.51 [c]
CD_2Cl_2	0.18	0.32	[a]

[a] decomposed.
[b] CD_3NO_2 was added to dissolve **3**.
[c] 25% of **3a**/**a'** decomposed.

The very similar ^{1}H NMR and UV−vis features of **3** and **3′** suggest that the new species **3′** is a diastereomer of **3**, where the configuration of the chiral spiro carbon atom is inverted, and the structure of the SP-H complex **3′b** has been verified by X-ray crystallography of a sample obtained by crystallization of a photolyzed sample from CH_2Cl_2−Et_2O at −30 °C (Figure 2), as discussed above. The inverted configuration at the C1 atom is evident as compared with **3a**,**c**.

Thus, UV irradiation of **3** causes inversion of the configuration of the spiro carbon atom, and the conversion can be interpreted in terms of the open intermediate **III**, which should result from heterolytic C−O bond cleavage of **3** induced by the UV irradiation (Scheme 4). In the subsequent ring closure of **III**, path *b* leading to **3′** should be kinetically favored over path *a* leading to **3**, because rotation of the phenolate group to the opposite side with respect to the RuCp* moiety can relieve the steric hindrance between the bulky RuCp* and phenolato parts. As for the reverse process (**3′** → **3**), judging from the results obtained, the ring opening of **3′** slowly proceeds even in the dark to regenerate **III**, which is converted to the thermodynamically more stable structure **3** with the electrostatic attractive interaction discussed above (Chart 2). In the case of the SP-H complex **3b**, a part of intermediate **IIIb** undergoes cis to trans isomerization of the olefinic part (path *c*), leading to the trans isomer **III′b**, which should be the colored species detected by UV−vis spectroscopy. Judging from the results, the rate of path *b* is greater than that of path *c*. The trans species **III′b** is rather stable at ambient temperature in the dark, but UV irradiation promotes the backward trans to cis olefin isomerization (path *d*) to finally afford **3′**.

The following features are noted for the photochemical behavior of the RuCp* adduct of the A ring in SP-X (**3**): (1) complexes **3** undergo photochemical ring opening of the spiro moiety to form the merocyanine form **III** in a manner similar to that for free SP (**1**), but (2) the dicationic Cp*Ru(η⁶-A ring) moiety in **III** is so electro-

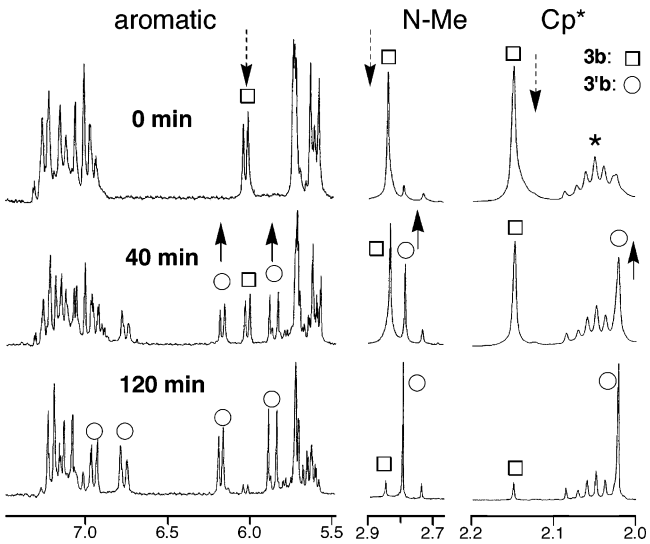

Figure 4. Changes of ^{1}H NMR spectra observed upon UV irradiation of **3b** (at 400 MHz in acetone-d_6). The asterisk denotes CD_3COCD_2H.

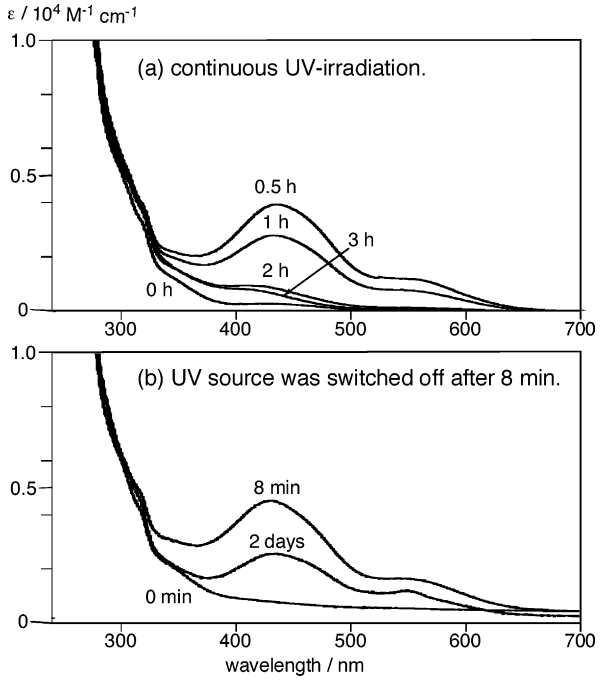

Figure 5. Changes of UV−vis spectra observed upon UV irradiation of **3b** (2.50×10^{-5} M, in CH_2Cl_2): (a) under continuous UV irradiation; (b) with the UV source switched off after 8 min.

Scheme 5

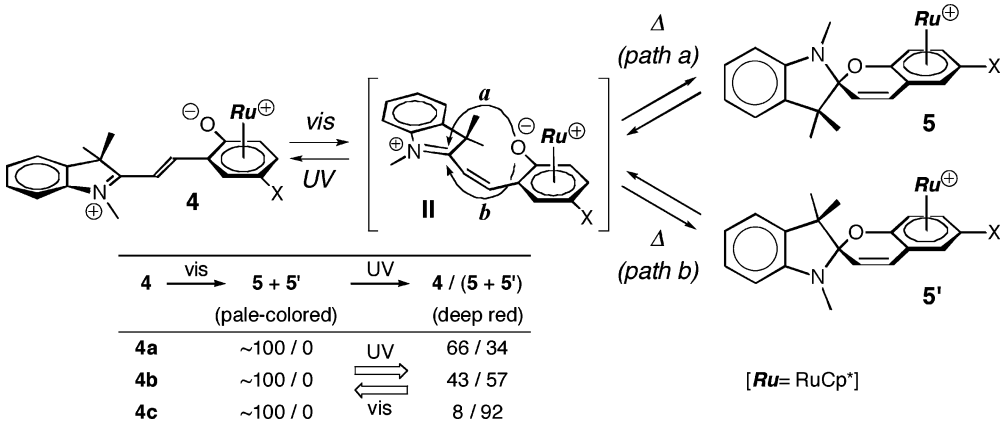

4	vis → 5 + 5' (pale-colored)	UV → 4 / (5 + 5') (deep red)
4a	~100 / 0	66 / 34
4b	~100 / 0	43 / 57
4c	~100 / 0	8 / 92

UV ⇌ vis

philic as to couple with the anionic phenolate moiety to readily regenerate the isomeric closed form **3′**, following the less sterically demanding pathway (path *b*), (3) the two ways of the ring-closing processes lead to the diastereomeric species **3** and **3′**, and (4) **3′** slowly reverts to **3** in the dark. In addition, (5) it is notable that the SP-H complex **3b** shows chromic behavior (**3/3′b** ↔ **III′b**), although the extent of formation of the colored species **III′b** is limited. The photochromic processes are based on the cis−trans isomerization of the olefinic parts in **IIIb** (cis) and **III′b** (trans). The forward process (**3b** → [**IIIb**] → **III′b**) is promoted by UV, and the decoloration (**III′b** → [**IIIb**] → **3b/3′b**) is promoted by UV and heat. The low photochromic performance should be ascribed to feature 2, which facilitates path *b* (to **3′b**) rather than path *c* (to **III′b**).

(ii) Photochromic Behavior of 4. Irradiation of the deep red complex **4** with a Xe lamp (visible light) caused decoloration to give a pale yellow solution (Scheme 5), and the decoloration process was monitored by ^{1}H NMR and UV−vis spectroscopy. As a typical example of the ^{1}H NMR change, the spectra for **4c** are shown in Figure 6, and the UV−vis spectral changes for **4a**−**c** are shown in Figure 7. Upon visible-light irradiation, the sharp ^{1}H NMR signals for the starting compound **4c** were replaced by the broad ones, suggesting formation of the new species **5**, which showed dynamic behavior. The broad signals were sharpened upon cooling at −30 °C and separated into two sets of signals in a 3:1 ratio, indicating that, at ambient temperature, the new species **5** was interconverted with another species **5′** at a rate comparable to the NMR coalescence time scale. On the basis of the pale color, **5/5′** were characterized as a pair of two diastereomers of the ring-closed species, a conclusion also supported by the chemical shifts of the *N*-Me groups (δ_H ~3 ppm) being comparable to those of **3/3′**, the adducts of the closed form (see, for example, Figure 3). The *N*-Me signals of the open species **4** appear at lower field (~4 ppm).

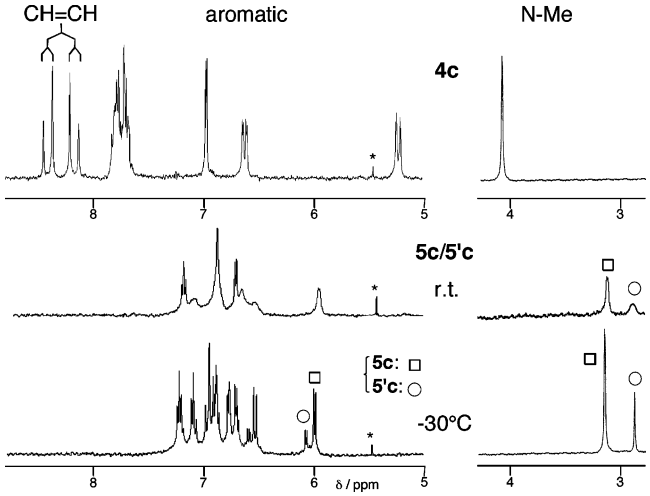

Figure 6. Changes of ^{1}H NMR spectra observed upon irradiation of **3c** with visible light (at 400 MHz in CD_3-NO_2). The asterisks denote residual CH_2Cl_2.

When the ring-closing process was monitored by UV−vis spectroscopy, visible light irradiation of CH_2Cl_2 solutions of **4** caused disappearance of the bands around 400 nm characteristic of the open form **4** accompanying isosbestic points, as can be seen from Figure 7a,d,g. The order of the decoloration rate is dependent on the substituent, and the half-lives for the colored species under visible light irradiation are roughly estimated as follows: 80 s (**4a**) > 40 s (**4b**) > 10 s (**4c**).

Subsequent UV irradiation of the equilibrated mixture of **5/5′** regenerated **4** to some extent, as can be seen from the UV−vis change (Figure 7b,e,h), and the system reached a photostationary equilibrated state, with the content of **4** being 66% (**4a**), 43% (**4b**), and 8% (**4c**). The ring-closing and -opening processes could be repeated by switching the light sources, i.e., visible light and UV, respectively, to show photochromic behavior (Figures 7c,f,i). A correlation between the decoloration rate of **5/5′** and the extent of the recovery of **4** is noted. Decoloration of the NO_2 derivative **4c** is very fast, but only 8% of **4c** is recovered upon UV irradiation of **5/5′c**, whereas decoloration of the OMe complex **4a** is 4 times slower than that of **4c** but two-thirds of **5/5′a** reverts to **4a** upon UV irradiation. Prolonged UV irradiation of **4c** gave a decomposition product, which lacked the A-ring part, as judged by ^{1}H NMR.

Thus, the B ring adduct **4** showed photochromic behavior between the colored, photostationary equilibrated state (**4** + **5/5′**) and the pale colored, closed form (**5/5′**).[13] The photochemical behavior can be interpreted by taking into account trans−cis isomerization of the olefinic part in **4**, as summarized in Scheme 5. Irradiation of the trans species **4** with visible light causes isomerization to the cis intermediate **II**, where the cationic iminium center and the anionic phenolate moiety are brought into proximity to couple with each

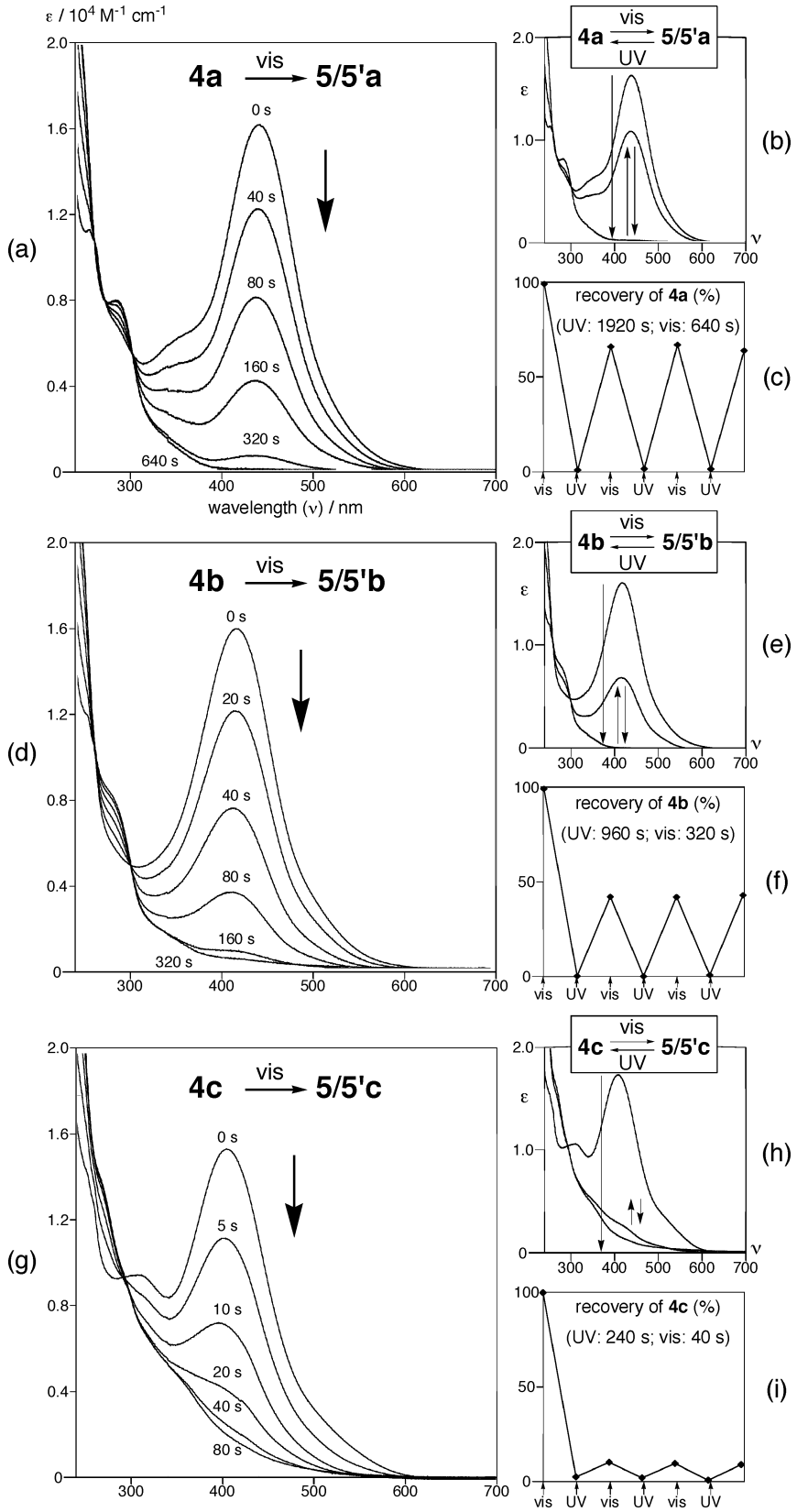

Figure 7. Changes of UV−vis spectra observed upon irradiation of **5/5′** with visible light (in CH_2Cl_2). Concentrations: [**4a**] = 2.49×10^{-5} M, [**4b**] = 2.72×10^{-5} M, [**4c**] = 2.50×10^{-5} M. Changes of UV−vis spectra observed upon visible light irradiation of (a) **4a** (2.49×10^{-5} M), (d) **4b** (2.72×10^{-5} M), (g) **4c** (2.50×10^{-5} M) (in CH_2Cl_2). Changes observed upon alternate UV and visible light irradiations of (b) **4a**, (e) **4b**, and (h) **4c**. Photochromic behavior of (c) **4a**, (f) **4b**, and (i) **4c**.

other and readily form the cyclic species **5** or **5′**. The two paths of the ring-closing processes lead to the two diastereomeric species with different configurations of the chiral spiro carbon atom (**5/5′**) in a manner similar to the stereoisomerism observed for **3/3′**. The dihydrobenzopyran ring in **5/5′**, however, readily opens to form **II**, because, in **II**, the anionic and cationic moieties can be stabilized by the electron-withdrawing effect of

Scheme 6

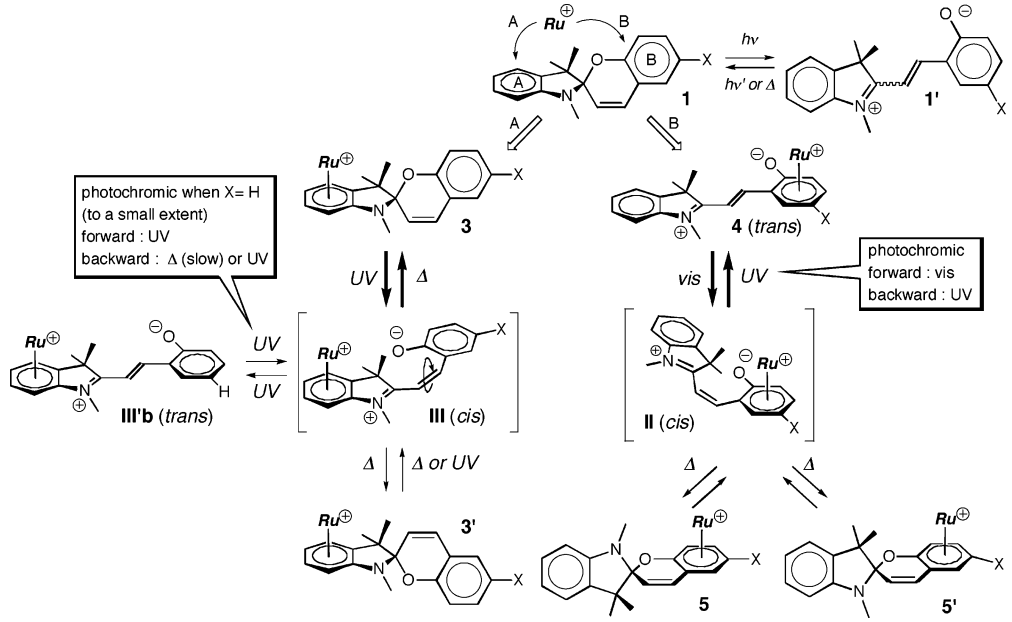

the RuCp*$^+$ fragment and delocalization over the A ring, respectively. The activation energy for the ring opening (**5/5′** → **II**) leading to the inversion of the chiral carbon atom is so low as to show the dynamic behavior (**5** ↔ **II** ↔ **5′**) at ambient temperature. Because **5** and **5′** could not be separated, definite characterization of the two species **5/5′** cannot be made and the major species is tentatively assigned to **5**, where the less bulky NMe moiety is projected to the Ru side.

The backward ring-opening process of **5/5′** is found to be promoted by UV irradiation, which should cause the cis to trans isomerization of the olefinic moiety in **II**. The backward process, however, is incomplete and a photostationary equilibrated state is established, presumably because the resultant open species **4** also absorbs UV light to partly undergo the forward ring -closing process. The substituent effect mentioned above may be interpreted in terms of this consideration. As can be seen from Figure 7a,d,g, the spectrum for **5/5′c** with virtually no absorption in the range of >300 nm is in contrast with that for **5/5′a** with substantial absorption up to 500 nm.

Conclusion. Complexation of the photochromic spirobenzopyran molecules **1** (SP-X) with the labile cationic ruthenium species [Cp*Ru(NCMe)$_3$]PF$_6$ (**2**) (Scheme 6) furnishes two isomers of the η^6-arene adducts [Cp*Ru(η^6-SP-X)]PF$_6$ (**3** and **4**): i.e., one of the two diastereomeric adducts of the A ring in the closed form of **1** (**3**; A) and the adduct of the B ring in the open merocyanine form of **1** (**4**; B).

UV irradiation of the pale yellow adduct **3** does not cause any apparent color change, but ^{1}H NMR monitoring reveals formation of the other diastereomer **3′** with the inverted configuration of the chiral spiro carbon atom, which gradually reverts to **3** when left at ambient temperature. The two diastereomers **3/3′** are interconverted with each other through the merocyanine form **III**, which should result from photochemical C−O bond heterolysis of **3** and **3′**. Photochromic behavior is noted for the SP-H complex **3b**, although the extent of the coloration is limited. UV irradiation of **3b** forms a small amount of the trans isomer of the merocyanine form (**III′b**; half-life ∼2 days) in addition to **3′b**, but upon further UV irradiation, **III′b** is finally converted into **3′**.

On the other hand, irradiation of the deep red adduct **4** with visible light causes trans to cis isomerization of the olefinic part to form an equilibrated mixture of the pale colored, closed diastereomers **5** and **5′**, which are interconverted under thermal reaction conditions at a rate comparable to the NMR coalescence time scale. Ring opening of **5/5′** readily occurs under thermal reaction conditions (even at ambient temperature) to form **II** but, in the resultant cis-open form **II**, the cationic and anionic centers in proximity readily undergo recombination to **5/5′**. UV irradiation of the closed form **5/5′** partly regenerates **4**, and as a result, the open merocyanine species **4** exhibits photochromic behavior between the photoequilibrated state (**4** + **5/5′**) and the closed forms (**5/5′**).

The aforementioned features of the present metal−SP-X combination system should result from addition of the cationic fragment, which perturbs the properties of the zwitterionic merocyanine form **1′**. For example, in the case of the A ring adduct **3**, the merocyanine form **III** should be destabilized by coordination of the cationic Ru fragment to the cationic part in **1′**, and as a result,

(13) (a) The complete isomerization of **4** into **5/5′** prompted us to examine photochemical switching of their physical properties. As a first attempt, the open SP-NO$_2$ complex **4c**, which exhibited the fastest photochemical response, was subjected to CV voltammetry. However, no significant result was obtained, because cyclic voltammograms of [Cp*Ru(η^6-alkylbenzene)]$^+$ complexes are rather featureless. Previous studies revealed that [Cp*Ru(η^6-alkylbenzene)]$^+$ complexes each showed one irreversible oxidation (>2.5 V) and reduction wave (−1.5 to −2.0 V),[13b] and highly functionalized arene complexes have not been studied so far. The open form **4c** showed one irreversible oxidation wave (0.92 V) and two reduction waves (−0.94, −1.60 V) (Figure S1; see the Supporting Information). UV irradiation of the sample caused a significant change of the voltammogram (one oxidation wave (0.64 V) and one reduction wave (−1.74 V) in addition to the reversible waves ($E_{1/2}$ = 0.28 V)) attributed to the open form **5/5′c**. Switching of the electrochemical properties is evident from the charts, but the assignments of the redox processes of **4c** and **5/5′c** could not be made. (b) Gusev, O. V.; Ievlev, M. A.; Peterleitner, M. G.; Pregudova, S. M.; Denisovich, L. I.; Petrovskii, P. V.; Ustynyuk, N. A. *J. Organomet. Chem.* **1997**, *534*, 57.

ring closure readily occurs to form the other closed species **3′**. On the other hand, the B-ring adduct of the merocyanine form (**4**) is stabilized through coordination of the anionic phenolate moiety and no ring closure is observed as long as **4** is protected from visible light. While the merocyanine form **1′** of SP-X can be detected by spectroscopic methods and, in the limited cases, can be isolated,[7,10] the isolation is not always easy, owing to the thermal backward reaction, and therefore, the properties of **1′** have yet to be studied. Because coordination of a cationic metal fragment to the B ring in **1′** causes a 100% conversion to the merocyanine form as described for **4**, metal complexation should serve as a versatile tool for the studies of the merocyanine form **1′**.

Another feature is diastereomerism arising from combination of the planar chirality of the Cp*Ru(η⁶-arene) moiety and the chiral spiro carbon atom (**3** vs **3′** and **5** vs **5′**).

Experimental Section

General Methods. All manipulations were carried out under an inert atmosphere by using standard Schlenk tube techniques. THF and ether (Na−K alloy), CH_2Cl_2 (P_2O_5), acetone ($KMnO_4$), and MeOH ($Mg(OMe)_2$) were treated with appropriate drying agents, distilled, and stored under argon. ^1H and ^{13}C NMR spectra were recorded on Bruker AC-200 (^1H, 200 MHz) and JEOL EX-400 spectrometers (^1H (VT, 2D), 400 MHz; ^{13}C, 100 MHz). Solvents for NMR measurements containing 0.5% TMS were dried over molecular sieves, degassed, distilled under reduced pressure, and stored under Ar. UV−vis and IR spectra (KBr pellets) were obtained on JASCO V570 and FT/IR 5300 spectrometers, respectively. ESI-mass spectra were recorded on a ThermoQuest Finnigan LCQ Duo mass spectrometer. UV and visible light irradiation were performed with an Ushio high-pressure mercury lamp (UM-452; $\lambda < 360$ nm with a U-360 cutoff filter) and a Soma Kogaku Xe lamp (150 W; $\lambda > 420$ nm with an L42 cutoff filter), respectively. Cyclic voltammograms were recorded on a BASi CV-50W voltammetric analyzer. SP-X (**1**)[14] and complex **2**[4h] were prepared by following the published procedures. Other chemicals were purchased and used as received. Chromatography was performed on silica gel.

Reaction of 1a with 2 (Preparation of 3a and 4a). Addition of **1a** (102 mg, 0.333 mmol) to a CH_2Cl_2 solution (15 mL) of **2** (153 mg, 0.302 mmol) caused a color change to red. After the mixture was stirred for 4 h at ambient temperature, the products were separated by column chromatography. Elution with CH_2Cl_2−MeOH (10/1) gave two bands, from which **3a** (96 mg, 0.139 mmol, 46% yield; pale yellow powders) and **4a** (85 mg, 0.124 mmol, 41% yield; deep red powders) were isolated after removal of the volatiles under reduced pressure. Complex **3a** was purified by recrystallization from CH_2Cl_2−Et_2O. Data for **3a** are as follows. ^1H NMR (CD_3NO_2; δ_H): Ar, 6.93 (1H, d, $J = 9.2$ Hz), 6.69 (1H, dd, $J = 8.8$ and 4.0 Hz), 6.64 (1H, d, $J = 4.0$ Hz); η⁶-Ar, 5.63 (1H, d, $J = 5.6$ Hz), 5.37 (1H, t, $J = 5.6$ Hz), 5.31 (1H, d, $J = 6.0$ Hz), 5.28 (1H, t, $J = 5.2$ Hz); CH=CH, 6.80 (1H, d, $J = 10.4$ Hz), 5.46 (1H, d, $J = 10.4$ Hz); 3.63 (3H, s, OMe), 2.63 (3H, s, NMe), 1.96 (15H, s, Cp*), 1.26, 1.07 (3H × 2, s × 2, CMe_2). $^{13}C\{^1H\}$ NMR (CD_3NO_2; δ_C): Ar + CH=CH + spiro C, 154.9, 147.1, 130.1, 123.5, 119.8, 119.6, 116.6, 115.8, 112.8; η⁶-Ar: 102.2, 101.5, 84.6, 82.6, 81.1, 72.0, 66.9; 95.7 (C_5Me_5), 56.0 (OMe), 52.0 (CMe_2), 39.4, 28.7, 28.0, 20.6 (Me), 10.6 (C_5Me_5). IR (cm^{-1}): 2964 (ν_{CH}), 839 (ν_{PF}). UV−vis (CH_2Cl_2; λ_{max}/nm ($\epsilon/M^{-1}\,cm^{-1}$)): 328 (4.3×10^3). ESI-MS (*m/z*): 545 ($M^+ - PF_6$). Anal. Calcd for $C_{30.5}H_{37}NO_2F_6PClRu$ (**3a**·$0.5CH_2Cl_2$): C, 50.11; H, 5.10; N, 1.92. Found: C, 50.32; H, 5.27; N, 2.13. Data for **4a** are as follows. ^1H NMR (CD_3NO_2; δ_H): *trans*-CH=CH, 8.35, 8.02 (1H × 2, d × 2, $J = 16.8$ Hz); Ar, 7.82 (1H, d, $J = 7.6$ Hz), 7.75 (1H, d, $J = 6.0$ Hz), 7.59 (2H, m); η⁶-Ar, 6.48 (1H, s), 5.94 (1H, m), 5.71 (1H, d, $J = 6.4$ Hz); 4.15 (3H, s, NMe), 3.73 (3H, s, OMe), 1.82 (6H, s, CMe_2), 1.81 (15H, s, Cp*). $^{13}C\{^1H\}$ NMR (CD_3NO_2; δ_C): Ar + CH=CH, 182.1, 148.6, 144.5, 143.1, 130.9, 130.3, 123.7, 116.6, 116.3; 96.4 (C_5Me_5); η⁶-Ar, 82.1, 77.4, 76.7, 71.8; 57.7 (OMe), 53.9 (CMe_2), 36.2, 26.3, 26.2 (Me), 10.2 (C_5Me_5). IR (cm^{-1}) 2974 (ν_{CH}), 1602 ($\nu_{C=O}$), 844 (ν_{PF}). UV−vis (CH_2Cl_2; λ_{max}/nm ($\epsilon/M^{-1}\,cm^{-1}$)): 441 (1.62×10^4). Despite several attempts an analytically pure sample could not be obtained.

Reaction of 1b with 2 (Preparation of 3b and 4b). The reaction (**1b** (144 mg, 0.518 mmol) + **2** (238 mg, 0.471 mmol)) was carried out in a manner similar to that described for **1a** (see above) and gave **3b** (149 mg, 0.226 mmol, 48% yield; pale yellow powders) and **4b** (133 mg, 0.202 mmol, 43% yield; deep red powders). Data for **3b** are as follows. ^1H NMR ($CDCl_3$; δ_H): Ar, 7.15 (1H, t, $J = 8.0$ Hz), 7.06 (1H, d, $J = 7.6$ Hz), 6.89 (2H, m); CH=CH, 6.81 (1H, d, $J = 9.6$ Hz); η⁶-Ar, 5.58 (1H, d, $J = 6.0$ Hz), 5.41 (1H, t, $J = 5.6$ Hz), 5.37−5.29 (2H, m, + CH=CH); 2.65 (3H, s, NMe), 1.98 (15H, s, Cp*), 1.27, 1.09 (3H × 2, s × 2, CMe_2). $^{13}C\{^1H\}$ NMR ($CDCl_3$; δ_C): 152.9, 130.3, 129.5, 127.7, 122.5, 121.5, 118.0, 117.9, 114.3 (arene), 101.4, 100.4 (η⁶-arene), 94.9 (C_5Me_5), 83.8, 81.7, 79.8, 65.9 (η⁶-arene), 51.2 (CMe_2), 28.5, 27.6, 19.6 (NMe and CMe_2), 11.3 (C_5Me_5). IR (cm^{-1}): 2963 (ν_{CH}), 840 (ν_{PF}). UV−vis (CH_2Cl_2): no characteristic band in the range of >240 nm. ESI-MS (*m/z*): 544 ($M^+ - PF_6$). Anal. Calcd for $C_{29}H_{34}NOF_6PRu$: C, 52.88; H, 5.20; N, 2.13. Found: C, 52.48; H, 5.02; N, 2.30. Data for **4b** are as follows. ^1H NMR (CD_3OD; δ_H): *trans*-CH=CH, 8.52, 8.20 (1H × 2, d × 2, $J = 16.4$ Hz); Ar, 8.03 (1H, d, $J = 7.6$ Hz), 7.79 (1H, d, $J = 6.4$ Hz), 7.58 (2H, m); η⁶-Ar, 6.41 (1H, d, $J = 5.2$ Hz), 5.81 (1H, d, $J = 6.4$ Hz), 5.77 (1H, t, $J = 5.2$ Hz), 5.64 (1H, t, 5.2 Hz); 4.12 (3H, s, NMe), 1.85 (15H, s, Cp*), 1.81, 1.80 (3H × 2, s × 2, CMe_2). $^{13}C\{^1H\}$ NMR (CD_3OD; δ_C): Ar + CH=CH, 183.6, 151.9, 144.7, 143.1, 131.0, 130.4, 123.8, 116.5, 116.3, 115.7; 96.0 (C_5Me_5); η⁶-Ar: 89.5, 86.2, 84.9, 84.7, 79.8; 53.9 (CMe_2), 36.1, 26.9 (Me), 11.3 (C_5Me_5). IR (cm^{-1}): 2962 (ν_{CH}), 1603 ($\nu_{C=O}$), 802 (ν_{PF}). UV−vis (CH_2Cl_2; λ_{max}/nm ($\epsilon/M^{-1}\,cm^{-1}$)): 420 (1.59×10^4). ESI-MS (*m/z*): 544 ($M^+ - PF_6$). Anal. Calcd for $C_{29}H_{34}NOF_6PRu$: C, 52.88; H, 5.20; N, 2.13. Found: C, 52.60; H, 4.98; N, 2.25.

Reaction of 1c with 2 (Preparation of 3c and 4c). The reaction (**1c** (147 mg, 0.456 mmol) + **2** (209 mg, 0.414 mmol)) was carried out in a manner similar to that described for **1a** (see above) and gave **3c** (236 mg, 0.335 mmol, 81% yield; pale yellow powders) and **4c** (44 mg, 0.062 mmol, 15% yield; deep red powders). Data for **3c** are as follows. ^1H NMR (CD_3NO_2; δ_H): Ar, 8.22 (1H, d, $J = 2.4$ Hz), 8.19 (1H, dd, $J = 7.2$ and 2.4 Hz), 7.37 (1H, d, $J = 8.8$ Hz); CH=CH, 7.26, 5.89 (1H × 2, d × 2, $J = 10.4$ Hz); η⁶-Ar, 6.09 (1H, d, $J = 6.0$ Hz), 5.80 (1H, d, $J = 6.4$ Hz), 5.76 (1H, t, $J = 6.0$ Hz), 5.65 (1H, t, $J = 8.0$ Hz); 2.87 (3H, s, NMe), 2.15 (15H, s, Cp*), 1.46, 1.29 (3H × 2, s × 2, CMe_2). $^{13}C\{^1H\}$ NMR (CD_3NO_2; δ_C): Ar, 161.3, 145.3, 131.4, 129.2, 126.2, 125.7, 124.1, 122.3, 118.8; η⁶-Ar, 106.6, 103.8, 87.4, 85.5, 83.7, 69.9; 98.5 (C_5Me_5); 55.3 (CMe_2), 31.4, 30.8, 22.7 (Me), 14.2 (C_5Me_5). IR (cm^{-1}): 2964 (ν_{CH}), 1339 (ν_{NO2}), 842 (ν_{PF}). UV−vis (CH_2Cl_2; λ_{max}/nm ($\epsilon/M^{-1}\,cm^{-1}$)): 264 (2.22×10^4), 318 (1.05×10^4). ESI-MS (*m/z*): 560 ($M^+ - PF_6$). Anal. Calcd for $C_{29.75}H_{35}N_2O_3F_6PCl_{1.5}Ru$ (**3c**·$(CH_2Cl_2)0.75$): C, 46.57; H, 4.53; N, 3.65. Found: C, 46.21; H, 4.96; N, 3.63. Data for **4c** are as follows. ^1H NMR (acetone-d_6; δ_H): *trans*-CH=CH, 9.02, 8.34 (1H × 2, d × 2, $J = 16.4$ Hz); Ar, 7.96 (1H, m), 7.88 (1H, m), 7.72 (2H, m); η⁶-Ar: 7.46 (1H, s), 6.93 (1H, d, $J = 6.8$ Hz), 6.31 (1H, d, $J = 7.2$ Hz); 4.28 (3H, s, NMe), 1.96, 1.93 (3H × 2, s × 2, CMe_2), 1.83 (15H, s, Cp*). $^{13}C\{^1H\}$ NMR (CD_3NO_2; δ_C): Ar + CH=CH, 183.7, 151.0, 149.7, 144.8, 143.1, 130.8, 130.1, 123.6, 116.2; 96.5 (C_5Me_5); η⁶-Ar: 107.7, 86.0, 85.2, 83.6,

(14) Torres, S.; Vázquez, A. L.; González, E. A. *Synth. Commun.* **1995**, *25*, 105.

Table 1. Crystallographic Data

	3a	**3c**	**3′b**
solvate			$^1/_2$ THF
formula	$C_{30}H_{36}NO_2F_6PRu$	$C_{29}H_{33}N_2O_3F_6PRu$	$C_{31}H_{42}NO_{1.5}F_6PRu$
formula wt	688.65	703.63	698.71
cryst syst	monoclinic	monoclinic	monoclinic
space group	$P2_1/c$	$P2_1/c$	$P2_1/c$
a/Å	8.733(1)	8.768(2)	20.340(10)
b/Å	18.407(4)	18.767(4)	8.751(6)
c/Å	18.103(4)	17.462(3)	17.114(8)
β/deg	93.03(1)	93.71(1)	93.16(3)
V/Å^3	2905.8(9)	2867.3(10)	3041(2)
Z	4	4	4
d_{calcd}/g cm^{-3}	1.574	1.630	1.526
μ/mm^{-1}	0.662	0.677	0.633
no. of diffractions collected	19 496	18 324	11 417
no. of variables	379	423	413
R1 for data with $I > 2\sigma(I)$	0.0474 (for 3910 data)	0.0881 (for 4729 data)	0.0960 (for 3536 data)
wR2	0.1349 (for all 6290 data)	0.2267 (for all 6455 data)	0.2641 (for all 5857 data)

80.0; 53.7 (CMe$_2$), 36.1, 26.2, 25.9 (Me), 9.60 (C_5Me_5). IR (cm^{-1}): 2962 (ν_{CH}), 1607 ($\nu_{C=O}$), 1341 (ν_{NO2}), 843 (ν_{PF}). UV−vis (CH_2Cl_2; λ_{max}/nm (ϵ/M^{-1} cm^{-1})): 312 (1.07×10^4), 406 (1.73×10^4). ESI-MS (m/z): 560 ($M^+ - PF_6$). Anal. Calcd for $C_{29}H_{33}N_2O_3F_6PRu$: C, 49.50; H, 4.73; N, 3.98. Found: C, 49.21; H, 4.96; N, 3.63.

UV Irradiation of 3 (Formation of 3′). Complex **3** dissolved in an appropriate deuterated solvent was irradiated with a Hg lamp, and the photochemical conversion was monitored by ^{1}H NMR. Characteristic ^{1}H NMR data for **3′** are as follows: **3′a**, δ_H (acetone-d_6) 3.75 (OMe), 2.76 (s, NMe), 1.99 (s, Cp*), 1.45, 1.33 (s × 2, CMe$_2$); **3′b**, δ_H (acetone-d_6) 7.20−7.00 (2H, m), 6.94 (1H, d, J = 3 Hz), 6.76 (1H, d. 3 Hz), 6.17 (1H, d, J = 2 Hz), 5.86 (1H, d, J = 4 Hz), 5.72 (1H, m), 5.60 (1H, m), 2.79 (3H, s, NMe), 2.02 (15H, s, Cp*), 1.46, 1.34 (3H × 2, s × 2, CMe$_2$); **3′c**, δ_H (CD_3NO_2) 2.79 (NMe), 2.12 (s, Cp*), 1.48, 1.36 (s × 2, CMe$_2$). The other signals for **3′a** and **3′c** could not be assigned, owing to the low conversions at the equilibrium.

Visible Light Irradiation of 4 (Formation of 5/5′). Complex **4** dissolved in an appropriate deuterated solvent was irradiated with a Xe lamp, and the photochemical conversion was monitored by ^{1}H NMR. UV−vis monitoring was carried out with nondeurated solvents. Characteristic ^{1}H NMR data for **5/5′** are as follows, and signals observed at ambient temperature were broad due to the dynamic behavior (see text): **5/5′a**, δ_H (acetone-d_6) 8.0−5.8 (m, Ar), 4.07 (3H, br s, OMe), 2.92 (3H, br s, NMe), 1.91 (15H, s, Cp*), 1.67, 0.96 (3H × 2, br s × 2, CMe$_2$); **5/5′b**, δ_H (acetone-d_6) 7.3−5.6 (m, Ar), 3.03 (3H, br s, NMe), 2.02 (15H, s, Cp*), 1.4−1.0 (br, CMe$_2$); **5/5′c**, δ_H (CD_3NO_2) 7.5−6.5 (br, Ar), 6.0 (br, Ar), 3.05 (br, NMe), 1.92 (s, Cp*), 1.0−1.5 (br, CMe$_2$). No characteristic UV−vis absorptions were detected, as can be seen from Figure 7.

X-ray Crystallography. Single crystals were obtained by recrystallization from **3a**,**c** (CH_2Cl_2−ether) and **3′b** (CH_2Cl_2−THF) and mounted on glass fibers. Diffraction measurements were made on a Rigaku RAXIS IV imaging plate area detector with Mo Kα radiation (λ = 0.710 69 Å) at −60 °C. Indexing was performed from three oscillation images, which were exposed for 3 min. The crystal to detector distance was 110 mm ($2\theta_{max}$ = 55°). In the reduction of data, Lorentz and polarization corrections and empirical absorption corrections were made.[15] Crystallographic data and results of structure refinements are listed in Table 1.

The structural analysis was performed on an IRIS O2 computer using the teXsan structure solving program system obtained from the Rigaku Corp., Tokyo, Japan.[16] Neutral scattering factors were obtained from the standard source.[17]

The structures were solved by a combination of the direct methods (SHELXS-86)[18] and Fourier synthesis (DIRDIF94).[19] Least-squares refinements were carried out using SHELXL-97[18] (refined on F^2) linked to teXsan. Unless otherwise stated, all non-hydrogen atoms were refined anisotropically, methyl hydrogen atoms were refined using riding models, and other hydrogen atoms were fixed at the calculated positions. **3c**: hydrogen atoms other than the methyl hydrogen atoms were refined isotropically. **3′b**: the NMe and CMe$_2$ parts of the five-membered ring containing N10 were found to be disordered and were refined by taking into account two components (0.59: 0.41). The THF solvate molecule (occupancy 0.5) was refined isotropically. Hydrogen atoms attached to the disordered parts and the THF solvate were not included in the refinement.

Acknowledgment. We are grateful to the Ministry of Education, Culture, Sports, Science and Technology of the Japanese Government and the Japan Society for Promotion of Science and Technology for financial support of this research.

Supporting Information Available: Tables giving crystallographic results and a figure giving a cyclic voltammograms of **4**c and **5/5′c**; crystal data are also given as CIF files. This material is available free of charge via the Internet at http://pubs.acs.org.

OM0506771

(15) Higashi, T. Program for absorption correction; Rigaku Corp., Tokyo, Japan, 1995.

(16) teXsan Crystal Structure Analysis Package, version 1.11; Rigaku Corp., Tokyo, Japan, 2000.

(17) *International Tables for X-ray Crystallography*; Kynoch Press: Birmingham, U.K., 1975; Vol. 4.

(18) (a) Sheldrick, G. M. SHELXS-86: Program for Crystal Structure Determination; University of Göttingen, Göttingen, Germany, 1986. (b) Sheldrick, G. M. SHELXL-97: Program for Crystal Structure Refinement; University of Göttingen, Göttingen, Germany, 1997.

(19) Beurskens, P. T.; Admiraal, G.; Beurskens, G.; Bosman, W. P.; Garcia-Granda, S.; Gould, R. O.; Smits, J. M. M.; Smykalla, C. The DIRDIF Program System, Technical Report of the Crystallography Laboratory; University of Nijmegen, Nijmegen, The Netherlands, 1992.